Pseudo-Random Testing and Signature Analysis for Mixed-Signal Circuits

Chen-Yang Pan and Kwang-Ting Cheng
Deptartment of Electrical and Computer Engineering
University of California, Santa Barbara

Abstract

In this paper, we address the problem of functional testing of mixed-signal circuits using pseudo-random patterns. By embedding the linear, time-invariant (LTI) analog circuit between a digital-to-analog converter (DAC) and an analog-to-digital converter (ADC), we can model the analog and converter circuitry as a digital LTI system and test it using the pseudo-random vectors. We give mathematical analysis and formulate the pseudo-random testing process as the linear transformation of a random process by the analog LTI device under test (DUT). We choose the first and the second moments of the transformed random process, which are closely related to the functionality of the DUT, as the signatures for fault detection. We show that such signatures can be estimated by proper arithmetic operations on the output responses of the DUT to the vectors generated by LFSRs. We illustrate and compare the effectiveness of several possible choices of signatures, through analysis and experimental results of several circuits, in terms of their fault detection capabilities and the testing hardware requirements.

I. Introduction

Mixed-signal circuits are gaining popularity in the applications such as telecommunications, multimedia, etc. A mixed-signal circuit typically includes some analog circuitry (amplifiers, filters, etc.), some digital circuitry (the DSP unit, control logic, etc.) and the converters (the ADC and the DAC). Due to the different types of circuitry involved, it usually requires several completely different testing schemes to test a mixed-signal chip. In general, testing methods for analog circuitry and converters have not achieved comparable maturity as those for digital circuitry. Recently several techniques for testing the analog circuitry [1-4] and the converters [5-7] have been reported. Most techniques do not use any fault model and essentially perform functional testing, which checks a set of parameters of the DUT to see if they fall within the tolerance range. There are two major issues for functional testing: (1) the design of input stimuli (test generation) and (2) the manipulation of the output response (signature analysis). The input stimuli could be sinewaves, square waves, DC signals, etc. and the output response could be interpreted in the time or frequency domain. For example, to check the bandwidth of a filter, we may apply a multitone signal, which is the summation of sinewaves with different frequencies, and perform the Fourier Transform on the output response to construct the signature. Here, how to choose the frequencies of the multitone signal is a 'test generation' problem and the Fourier Transform is used to perform the 'signature analysis'. In [8], a signature analyzer for analog and mixed-signal circuits, considering the imprecise nature of analog signals, is proposed.

A Built-In Self-Test (BIST) structure for mixed-signal circuits is proposed in [9]. The digital portion of the DUT is tested by using known methods (e.g., the pseudo-random technique). Also, by embedding the analog portion between a DAC and an ADC, the analog portion can be tested using digital signals. Based on a similar testing configuration, we propose and thoroughly analyze the pseudo-random testing technique for mixed-signal circuits. We model the analog LTI circuit, when embedded between the converters, as a digital LTI system. By applying pseudo-random patterns generated from the LFSRs and providing proper manipulation on the output response (both are done digitally), we can perform functional testing on the embedded analog DUT. Because the flat spectrum of the pseudo-random signal essentially contains infinite number of tones, we can use it as a universal stimulus for any LTI circuit. Therefore, as opposed to other functional testing methods (e.g., the multitone method), we have alleviated the test generation problem.

In testing analog LTI circuits using the pseudo-random technique, the input stimulus can be viewed as a random sequence generated by a random process. The output sequence of the DUT is also a random sequence generated by another random process. The output random process can be viewed as a linear transformation, performed by the DUT, from the input random process [10,11]. Because there exists a mathematical relationship between the moments of the input/output random processes and the functionality of the DUT, we can fully characterize the DUT if the moments of the random processes can be obtained. As will be shown in Sec.III, we use the first and second moments, i.e., the mean, the auto-correlation and the cross-correlation, to characterize the DUT and these quantities can be estimated from the input/output random sequences using common arithmetic operations. For example, we can construct the impulse responses at selected time instances of the LTI system by obtaining the 'cross-correlation' between the input and output sequences. Because the impulse response fully characterizes a LTI system, we can use the constructed impulse response as the signature to determine the correctetness of the DUT. Note we may construct different signatures by different ways of manipulation on the output response. These signatures may have different fault detection capability, hardware requirements and testing time. We will compare these differences in Sec.IV and Sec.V.

This paper is organized as follows. Sec.II describes how the analog LTI circuit is modeled as a digital LTI system when embedded between the converters. Sec.III shows the mathematical relationship between the first and second moments and the impulse response of the DUT. Sec.IV shows the hardware realization of the pseudo-random scheme. In Sec.V, we use the analog filters and a converter to demonstrate the pseudo-random technique for various signatures. In Sec.VI, we give some detailed discussion on the fault detection capability of the signatures.

II. Modeling of an Analog LTI Circuit as a Digital LTI System

Fig.1 shows how we can model an analog LTI circuit as a digital LTI system. The analog circuit with impulse response $h(t)$ is embedded between a DAC and an ADC. The DAC converts the digital input $x[n]$ into an analog signal $x(t)$ (we assume the input $x[n]$ is not interpolated and therefore $x(t)$ are successive analog rectangular pulses). The the response $y(t)$ is sampled by the ADC and converted into digital signal $y[n]$. The digital signals $x[n]$ are applied at a rate of F_s (= $1/T_s$), which is equal to the sampling rate of the ADC. Note that the input sequence $x[n]$ and the output sequence $y[n]$ are defined at time instances $t=nT_s$, where $n=0,1,2,...,\infty$. If the signal $y(t)$ varies slowly during each sampling interval $[nT_s, (n+1)T_s]$, it can be shown [10] that the impulse response $h[n]$ of the modeled digital LTI system is equal to $T_s \bullet h(nT_s)$. If the DAC and the ADC is of size B-bit, the ratio between the mean square values of the quantization error $e[n]=y[n]-y(nT_s)$ and the input signal $y(nT_s)$ (assuming $y(nT_s)$ is random, uniformly distributed over the full-scale V_s of the ADC) is roughly $1/2^B$. For example, if we use 10-bit converters, the quantization error, in the mean square sense, is roughly 0.1% of the input signal.

We can describe the functionality of a digital LTI system in either the z-domain (with the transfer function $H(z)$) or the discrete-time domain (with the impulse response $h[n]$). In the discrete-time domain, the output $y[n]$ of a causal LTI system ($h[n]=0$ for $n<0$) with impulse response $h[n]$, given the input $x[n]$ (deterministic or random), is

$$y[n] = \sum_{k=0}^{\infty} x[n-k] \bullet h[k] \qquad Eq.(1)$$

Here we assume the LTI system is causal, which is the property for any system to be physically realizable. We also assume that the LTI system is stable (the output $y[n]$ cannot grow to infinity as long as the input $x[n]$ is finite). The stability of the system guarantees that the signatures to be discussed in the subsequent sections are always finite.

III. Mathematical Analysis

A random process X (discrete-time) can be viewed as a process which generates the random sequence $x[n]$ (we assume $n \geq 0$) with certain probability distribution. The random sequence $x[n]$ may be mutually independent (i.e., white noise) or have some correlation between one another. A stationary random process implies that the probability density $f_{x[n]}$ for each random variable $x[n]$ is identical. In other words, the characteristics of the random process which generates the random sequence $x[n]$ do not change with time. For example, the random sequence $x[n]$ generated by the LFSR is stationary and possesses the white noise property (if the period of the random sequence is long enough). When a stationary, white noise sequence $x[n]$ passes a LTI system, the resulting output random sequence $y[n]$ is also stationary but not necessarily possesses the white noise property.

In pseudo-random testing for an analog LTI circuit, the input stimulus $x[n]$ is a random sequence generated by a specific random process X. When the random sequence $x[n]$ passes a LTI system, a new random process Y, which generates the random sequence $y[n]$, is formed at the output. Because Eq.(1) is valid for either deterministic or random signals, we can determine the output sequence $y[n]$ if $x[n]$ is given. Note that any functional fault which changes the impulse response $h[n]$ will change the output sequence $y[n]$.

III-1 Relationships Between Moments and $h[n]$

In the following we will derive the mathematical relationship between the first and second moments of a random process and the impulse response of a LTI system. As will be shown in this subsection, the first and second moments of a random process can be expressed as the impulse response 'compressed' in certain manner. We first show the definitions of the first and second moments of a random process

$$m_x[n]=E\{x[n]\} \qquad Eq.(2)$$

$$R_x[n_1,n_2]=E\{x[n_1] \bullet x[n_2]\} \qquad Eq.(3)$$

$$R_{xy}[n_1,n_2]=E\{x[n_1] \bullet y[n_2]\} \qquad Eq.(4)$$

where $x[n]$ and $y[n]$ is the random sequence generated by the random process X and Y. The sequence $m_x[n]$ in Eq.(2) is formed by taking the mean of the random variable $x[n]$ (the first moment). Eqs.(3)-(4) are called the 'auto-correlation of the random process X' and the 'cross-correlation between the random processes X and Y' respectively (the second moments). If the random processes X and Y are stationary and we assume $n_2-n_1=m$, Eqs.(2)-(4) become

$$m_x[n]=m_x \qquad Eq.(5)$$

$$R_x[n_1,n_2]=R_x[m] \qquad Eq.(6)$$

$$R_{xy}[n_1,n_2]=R_{xy}[m] \qquad Eq.(7)$$

Eqs.(5)-(7) show that for a stationary random process, the first moment m_x (m_y) is constant and the second moments $R_x[m]$ ($R_y[m]$) and $R_{xy}[m]$ depend only on the distance m between the time instances of the two random variables $x[n_1]$ and $x[n_2]$. It can also be shown [11] that the auto-correlation function is even ($R_x[m]=R_x[-m]$, $R_y[m]=R_y[-m]$).

To see the relationship between the functionality ($h[n]$) and the first and second moments of the stationary output random process Y (assuming the input random process X is stationary), we take the expectation on both sides of Eq.(1) and use the stationary property of $x[n]$ and $y[n]$

$$m_y=E\{y[n]\}=\sum_{k=0}^{\infty} E\{x[n-k]\}h[k]= m_x \sum_{k=0}^{\infty} h[k] \qquad Eq.(8)$$

Similarly, the auto-correlation function for the output random process Y is

$$R_y[m]=E\{y[n] \bullet y[n+m]\}=E\{\sum_{k=0}^{\infty}\sum_{r=0}^{\infty} x[n-k] \bullet h[k] \bullet x[n+m-r] \bullet h[r]\}$$

$$=\sum_{k=0}^{\infty} h[k] \sum_{r=0}^{\infty} h[r] \bullet E\{x[n-k] \bullet x[n+m-r]\} = h[k] \sum_{r=0}^{\infty} h[r] \bullet R_x[m+k-r] \qquad Eq.(9)$$

When the input sequence $x[n]$ possesses the white noise property and $m_x=0$, the auto-correlation function $R_x[m]=\sigma_x^2 \bullet \delta[m]$,

where σ_x^2 denotes $E\{x[n]^2\}$. Therefore, Eq.(9) becomes

$$R_y[m] = \sum_{r=0}^{\infty} h[k]\bullet h[k+m] \qquad Eq.(10)$$

Note that $R_y[0]$ is simply the summation of the square of the impulse response (the energy of the LTI system). Due to the hardware requirement (will be explained in Sec. IV), we only use $R_y[0]$ as the signature. The cross-correlation between the random processes X (white noise with zero mean) and Y is

$$R_{xy}[m] = E\{x[n]\bullet y[n+m]\} = E(x[n] \sum_{k=0}^{\infty} x[n+m-k]\bullet h[n+m])$$
$$= \sum_{k=0}^{\infty} h[k]\ E(x[n]\bullet x[n+m-k]) = h[m]\ \sigma_x^2 \qquad Eq.(11)$$

The relationship between the functionality of the LTI system (the impulse response) and moments of the random processes X and Y are established by Eqs.(8), (10) and (11). **Therefore, we can use the mean m_y, the auto-correlation $R_y[m]$ and the cross-correlation $R_{xy}[m]$ as the signatures to test a LTI system by applying the white noise $x[n]$.** As can be shown in subsequent sections, the three signatures have different fault detection capabilities and hardware requirements.

III-2 Computation of the Signature

To make the pseudo-random scheme practical, the expectation operation on the random variables ($y[n]$, $y[n]\bullet y[n+m]$ and $x[n]\bullet y[n+m]$ in Eq.(8), (10) and (11) respectively) should be replaced by the 'time averaging' operation. That is, we use finite number (N) of samples observed during certain finite time interval to estimate the expectations of the random variables. Therefore, the signature thus obtained (also a random variable) is an estimate of the derived signature. The mean of the estimated signature is equal to the derived signature and we should make the standard deviation of the estimated signature as small as possible such that a certain confidence level is achieved for fault detection. The 'time averaging' operation (we denote as < >) used to obtain the estimated signature can be carried out easily. The fact that the mean of the 'time averaged' random variable is equal to the mean of the random variable itself is shown as follows.

$$E\{<g[n]>\} = E\{\frac{1}{N}\sum_{i=0}^{N-1} g[i]\} = \frac{1}{N}\sum_{i=0}^{N-1} E\{g[i]\} = m_g \qquad Eq.(12)$$

, where $g[n]$ denotes any random sequence generated by a stationary random process and m_g is the mean of $g[n]$. For clarity, we denote the estimate of the derived signatures m_y, $R_y[m]$ and $R_{xy}[m]$ as $\overline{m}_y$, $\overline{R}_y[m]$ and $\overline{R}_{xy}[m]$ respectively. By replacing $g[n]$ in Eq.(12) with $y[n]$, $y[n]\bullet y[n+m]$ and $x[n]\bullet y[n+m]$, we can show $E\{\overline{m}_y\}=m_y$, $E\{\overline{R}_y[m]\}=R_y[m]$ and $E\{\overline{R}_{xy}[m]\}=R_{xy}[m]$.

III-3 Fault Detection Using the Signatures

Because the estimated signatures $\overline{m}_y$, $\overline{R}_y[m]$ and $\overline{R}_{xy}[m]$ are random variables, in addition to knowing the expectations, we need know the standard deviations such that the fault-free ranges can be defined. However, an analytical form for the relationship between the standard deviations of the estimated signatures $\overline{m}_y$, $\overline{R}_y[m]$ and $\overline{R}_{xy}[m]$ and the number of random patterns (N) is extremely difficult to derive. From the simulation results we know (1) the probability distributions of the output sequences $y[n]$, $y[n]\bullet y[n+m]$ and $x[n]\bullet y[n+m]$ are close to the Gaussian distribution and (2) the standard deviations of the estimated signatures are approximately proportional to the inverse square root of N. Therefore, we can reduce the difference between the derived and estimated signatures (enhancing the fault detection capabilities of the signatures) by applying more random patterns, which is subject to the testing budget. Also, we choose the $3\sigma_g$ range $[m_g-3\sigma_g\ , m_g+3\sigma_g]$ as the fault-free range (this range corresponds to a 99.5% confidence level if the random variable $g[n]$ (= $y[n]$, $y[n]\bullet y[n+m]$ or $x[n]\bullet y[n+m]$) approaches the Gaussian distribution). Note that for a practical purpose, instead of obtaining the signature range of the DUT $[m_{g,DUT}-3\sigma_{g,DUT}\ , m_{g,DUT}+ 3\sigma_{g,DUT}]$ to see if the derived fault-free signature m_g falls within this range (claimed as fault-free), we simply obtain the estimated signature $\overline{m}_{g,DUT}$ of the DUT to see if it falls within the range $[m_g-3\sigma_g\ , m_g+3\sigma_g]$. The fault-free range $[m_g-3\sigma_g\ , m_g+3\sigma_g]$ corresponding to specific number of random patterns N needs to be pre-calculated and the estimated signature $\overline{m}_{g,DUT}$ is obtained by processing the output responses of the DUT to the N random patterns.

IV. Hardware Realization for the Pseudo-Random Testing Technique

Fig.2(a)-(c) show the possible hardware realizations of the pseudo-random testing technique using the signatures $\overline{m}_y$, $\overline{R}_y[0]$ and $\overline{R}_{xy}[m]$ respectively. The analog LTI circuit is modeled as a digital LTI system by embedding it within the DAC and the ADC. The random pattern generator LFSR1 generates the input stimulus $x[n]$ and the output sequence $y[n]$ is processed by the arithmetic unit. Without including the DAC and the ADC, the hardware requirements for constructing the signatures $\overline{m}_y$, $\overline{R}_y[0]$ and $\overline{R}_{xy}[m]$ are as follows.

- $\overline{m}_y$ - a LFSR (LFSR1) and an adder (without scaling the final sum by N)
- $\overline{R}_y[0]$ - a LFSR (LFSR1), an adder and a multiplier
- $\overline{R}_{xy}[m]$- two LFSRs (LFSR1 and LFSR2), an adder and a multiplier

In Fig.2(a), the signature $\overline{m}_y$ is constructed by summing up N output data $y[n]$. In Fig.2(b), the output data $y[n]$ are first squared and then summed up to obtain the signature $\overline{R}_y[0]$. The signature $\overline{R}_{xy}[m]$, as shown in Fig.2(c), is constructed by multiplying $y[n]$ with the delayed version of the input sequence $x[n-m]$ and summing up the products $y[n]\bullet x[n-m]$. Note that for every distinct delay m, we can construct the signature $\overline{R}_{xy}[m]$ by programming the LFSR2 without adding any delay elements. However, to construct the signature $\overline{R}_y[m]$ for different m's, multiple delay elements are required and this turns out to be impractical when m becomes large (if we need more signatures for fault-detection). Therefore, only the auto-correlation of zero delay $\overline{R}_y[0]$ is used for fault detection.

Because the DAC, the ADC and the DSP unit are common elements in a mixed-signal chip, limited amount of extra

hardware is required for the BIST realization. The first and second moments of a random process, which we choose as the signatures, can be easily computed by properly programming the DSP unit.

V. Simulation Results

In this section we show results to compare the effectiveness (that is, fault detection capability) of the three signatures: the mean m_y, the auto-correlation $R_y[0]$ and the cross-correlation $R_{xy}[m]$. The analog LTI circuits used for experiments are shown in Fig.3(a)-(d). Circuit X1 and X2 are low-pass filters with 3 poles (bandwidth 1KHz) and 5 poles (bandwidth 100Hz) respectively. Circuit X3 is a notch filter with 2 zeros and 2 poles (notch bandwidth from 55Hz to 65Hz). Circuit X4 is a 4-bit DAC (highlighted). Circuits X1, X2 and X3 are tested using the configurations in Fig.2(a)-(c) with the converters of size 10-bit at the sampling rate F_s=1MHz. Fig.3(d) shows how the circuit X4 can be tested. Note that the configurations for construction of the three signatures are similar to Fig.2(a)-(c) except that the 10-bit ADC is not required. The output of the 4-bit ADC is combined with a 6-bit all-zero pattern to incorporate the quantization error. The 10-bit signal $y[n]$ thus formed is connected directly to the arithmetic unit for signature analysis. Note that the impulse response for the DAC-ADC digital module is an unit impulse $\delta[m]$.

Table 1(a)-(c) shows the faults *f1-f5*, *f6-f10* and *f11-f15* we considered for circuit X1, X2 and X3 respectively. The column 'deviation' shows the amount of deviation of the passive components from their nominal values in terms of percentage. For example, 'C_1: +20%' of *f1* means the value of the component C_1 in circuit X1 increases by 20% and therefore the faulty value becomes 16.70nF (the nominal value is 13.92nF). For circuit X4, three faults *f16* (the nonlinearity error), *f17* (the gain error) and *f18* (the offset error) were considered. The input/output transfer curves for the fault-free and the faulty ADCs are shown in Fig.4(a)-(d).

When we apply the random sequence $x[n]$ to test the circuits X1-X4, the all-zero pattern is interpreted as '-1' and the all-one pattern is interpreted as '1'. However, according to Eq.(8), if the mean of $x[n]$ is zero, the mean of the estimated signature $\overline{m}_y$ will be zero for the faulty and fault-free DUTs. Therefore, we interpret the all-zero pattern and the all-one pattern as '0' and '1' respectively (m_x=0.5) when constructing the signature $\overline{m}_y$.

Table 2(a)-(d) shows the fault detection capability of the three signatures m_y, $R_{xy}[m]$ and $R_y[0]$ for circuit X1(N=128K), X2(N=256K), X3(N=256K) and X4(N=16K). The row 3σ in each table is the 'uncertainty' of the fault-free signature estimated by the associated number of random patterns N. The row Δ_f stands for the difference between the 'mean of the estimated signature of the faulty circuit' and the 'derived fault-free signature'. That is, $\Delta_f = E\{\overline{R}_{xy,DUT}[m]\}$ - $R_{xy}[m]$, $E\{\overline{R}_{y,DUT}[0]\}$ - $R_y[0]$ and $E\{\overline{m}_{y,DUT}\}$ - m_y for the entries under column $R_{xy}[m]$, $R_y[0]$ and m_y respectively. The quantities $E\{\overline{R}_{xy,DUT}[m]\}$, $E\{\overline{R}_{y,DUT}[0]\}$ and $E\{\overline{m}_{y,DUT}\}$ are obtained by applying 100 independent sets of N random patterns. In the actual testing process, however, we only apply one set of N random patterns for fault detection. The fault f is detected if $|\Delta_f|$ is less than the 3σ value in the same column and the detected faults are highlighted. For example, *f1* in circuit X1 can be detected by the signatures $R_{xy}[200]$ and $R_y[0]$. From the simulation results, we also found that σ is roughly proportional to the inverse square root of N. Therefore, by enhancing the number of random patterns from 128K to 512K (reducing the value of σ by half) *f1* can also be detected by $R_{xy}[400]$, $R_{xy}[800]$, $R_{xy}[1000]$ and $R_{xy}[1200]$.

From Table 2(a)-(d), the signature m_y can hardly detect the faults in circuits X1, X2 and X3 but it has comparable detection capability to $R_{xy}[m]$ and $R_y[0]$ for circuit X4. Also, by changing the delay time m in LFSR2, we can use $R_{xy}[m]$ at different m's for fault detection. Therefore, to enhance the fault detection capability of $R_{xy}[m]$, we can try (1) increasing the number of random patterns N or (2) using more signatures at different m's. For circuit X1, X2 and X3, we use six $R_{xy}[m]$'s. To detect all the five faults *f1-f5* in circuit X1, $R_{xy}[m]$ needs $6N$ (N=128K) random patterns while $R_y[0]$ needs $36N$ random patterns. Similarly, for the faults *f6-f10* and *f11-f15*, $R_{xy}[m]$ needs $12N$ (N=256K) random patterns and $R_y[0]$ needs $4N$ random patterns. For faults *f16-f18* in circuit X4, $R_{xy}[m]$ needs roughly four times of the random patterns required by $R_y[0]$ even we only use $R_{xy}[0]$ as the signature.

Note that some hard-to-detect faults by signature $R_y[0]$ is not necessarily difficult to be detected by $R_{xy}[m]$ and vice versa. For example, the faults *f3* and *f5*, which make $R_y[0]$ seemingly less efficient than $R_{xy}[m]$, are the most easily detectable faults for $R_{xy}[m]$. Therefore, if two multipliers are available, by constructing the signatures $R_{xy}[m]$ and $R_y[0]$ concurrently for fault detection, the testing time can be reduced.

VI. Discussions and Comparisons of the Signatures

For a stable LTI system, the impulse response $h[n]$ decays to zero when n approaches infinity. According to the Fourier Transform relationship, the significant portion of the impulse response is roughly bounded by the time interval $[0, t_0]$, where t_0 is roughly equal to π/BW (BW denotes the 3-db bandwidth of the LTI system). In terms of the discrete-time index n (or m), the time interval is $[0, n_0]$, where $n_0=t_0/T_s$. According to Eq.(1), only the significant portion of $h[n]$ contributes to the output $y[n]$. Therefore, if we use $R_{xy}[m]$ as the signature, we need only to investigate one or more $R_{xy}[m]$'s where $0 \le m \le n_0$.

Fig.5 shows the impulse response for the fault-free (solid line) and the faulty, *f6*, (dotted line) circuit X2. The observation time in Fig.5 (from 0 to 0.04 sec) corresponds to the discrete-time index m from 0 to 40000 (by the relationship $t=m \bullet T_s$, where T_s=1μs). The significant portion of the impulse response in Fig.5 is bounded by [0, 31400] in terms of m. If we want to use, for example, $R_{xy}[31400]$ as the signature, we will need 31400+N clock cycles. The amount of delay m may be nontrivial with respect to N. This problem becomes worse when the bandwidth of the DUT is low, that is, the speed of the DUT is slow. For example, to test a 10Hz device, the delay time required could be as long as 0.3 sec. Therefore, if we want to reduce the testing time by increasing the clock rate F_s, there

is an lower bound placed by the speed of the DUT. The property that the testing time using $R_{xy}[m]$ as the signature is dependent on the speed of the DUT is undesirable. The signatures $R_y[0]$ and m_y have no such problem because no delay is needed.

From the simulation results, we also found the signature m_y has significantly lower detection capability than $R_{xy}[m]$ and $R_y[0]$ for circuit X1, X2 and X3. The low detection capability of m_y can be explained by Eq.(8) and Fig.5. From Eq.(8) we know the deviation Δ_f is the summation of the differences between $h_f[n]$ and $h[n]$. Fig.5 shows that for fault *f6*, the differences to be summed tend to cancel out and therefore the final deviation Δ_f is small. We have observed similar phenomenon for faults *f1-f15*. However, for faults *f16-f18*, the only significant difference between $h_f[n]$ and $h[n]$ occurs at n=0 (the impulse response is $\delta[m]$) and therefore the fault-cancellation phenomenon does not occur. Similar fault-cancellation phenomenon could happen to $R_y[0]$ but is much less distinguished. If we assume the faulty output sequence is $y_f[n]= y[n]+\delta y[n]$, the difference between $y_f[n]^2$ and $y[n]^2$ is $2\delta y[n]\bullet y[n]+\delta y[n]^2$ and the term $\delta y[n]^2$ is always summed up in Δ_f without cancellation.

For circuit X4, the detection capability of $R_y[0]$ and m_y is better than $R_{xy}[m]$. This can be explained as follows. We assume the output $y_f[n]=y[n]+\delta y[n]$ and we know $x[n]=y[n]$ for the fault-free circuit (excluding the quantization noise). The final differences Δ_f for the signatures m_y, $R_{xy}[m]$ and $R_y[0]$ are constructed by summing up the quantities $y_f[n]-y[n] = \delta y[n]$, $y_f[n]\bullet y[n] - y[n]^2 = \delta y[n]\bullet y[n]$ and $y_f[n]^2 - y[n]^2 = 2\delta y[n]\bullet y[n] + \delta y[n]^2$ respectively. It can be seen that Δ_f for $R_y[0]$ is roughly two times of the Δ_f for $R_{xy}[m]$. Also, because $y[n]$ varies uniformly between [0,1] (the average is about 0.5), we can expect that the Δ_f for m_y is roughly two times of the Δ_f for $R_{xy}[m]$.

VII. Conclusions

We have provided mathematical analysis, hardware implementation schemes and experimental results for several signature analysis methods for testing mixed-signal circuits using the pseudo-random technique. We model the analog LTI circuit as a digital LTI circuit such that the stimuli generation and signature analysis can be performed digitally. We then employ the concept of the linear transformation on a random process and use the mean (m_y), the auto-correlation ($R_y[0]$) and the cross-correlation ($R_{xy}[m]$) as the signatures. By proper arithmetic operations on the output random sequence generated by the output random process of the DUT, we have constructed the signatures which are closely related to the functionality of the DUT. The hardware required for the testing scheme is usually available on a DSP-based mixed-signal chip. For such chips, these techniques can be used for a BIST implementation. For other circuits that don't have a DSP unit on chip, these methods can be used for external testing and the testing hardware can be included in the tester. We have shown by analysis and simulation results that the fault detection capability for the signatures $R_{xy}[m]$ and $R_y[0]$ are comparable but $R_y[0]$ requires less hardware. The signatures $R_y[0]$ and m_y for testing the DAC and the ADC are better than $R_{xy}[m]$ in terms of the number of random patterns required. In general, the fault-cancellation phenomenon results in the low detection capability of m_y.

Reference

[1] N. Nagi and J. A. Abraham. "Hierarchical fault modeling for analog and mixed-signal circuits", *VLSI Test Symposium*, Apr. 1994, pp. 96-101

[2] N. Nagi, A. Chatterjee, A. Balivada and J. A. Abraham. "Fault-based automatic test generator for linear analog circuits", *International Conference on CAD*, Nov. 1993, pp. 88-91

[3] M. Soma, "A Design-For-Test Methodology for Active Analog Filter", *Internationl Test Conference,* Oct. 1993, pp. 183-192

[4] F. Bouwman, et al. "Application of Joint Time-Frequency Analysis in Mixed-Signal Testing", *International Test Conference*, Oct. 1994, pp.747-756

[5] K. Arabi, B. Kaminska, J. Rzeszut. "A New Built-In Self-Test Approach for Digital-to-Analog and Analog-to-Digital Converters", *International Conference on CAD*, Nov. 1994, pp.491-494

[6] M. Toner, G. Roberts. "A BIST Scheme for an SNR Test of a Sigma-Delta ADC", *International Test Conference*, Oct. 1993, pp.805-814

[7] E. Teraoka, et al. "A Built-In Self-Test for ADC and DAC in a Single-Chip Speech CODEC", *Internationl Test Conference*, Oct. 1993, pp.791-796

[8] N. Nagi, A. Chatterjee and J. A. Abraham, "A Signature Analyzer for Analog and Mixed-signal Circuits", *International Conference on Computer Design,* 1994, pp. 284-287

[9] M. Ohletz, "Hybrid Built-In Self-Test for Mixed Analog/Digital Integtated Circuits", *European Test Conference*, Apr. 1991, pp. 307-316

[10] A. Oppenheim, R. Schafer. "Discrete-time Signal Processing", Prentice-Hall, 1989

[11] C.W. Therrien. "Discrete Random Signals and Statistical Signal Processing", Prentice-Hall, 1992

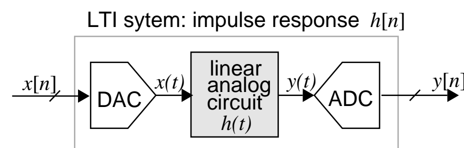

Fig.1 Modeling an analog LTI circuit as a digital LTI system

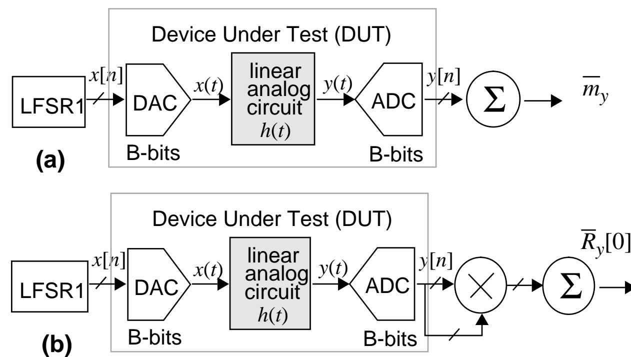

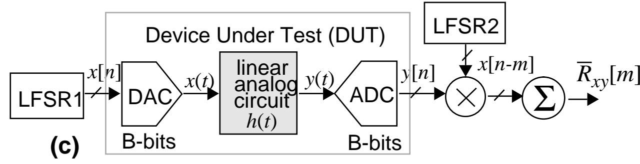

Fig.2 Hardware realizations of the pseudo-random testing scheme by using the signatures (a)$\overline{m}_y$ (b)$\overline{R}_y$[0] (c)$\overline{R}_{xy}$[m]

faults	deviation
f1	C_1: +20%
f2	R_1: +20%
f3	R_3: -20%
f4	C_2: -20%
f5	C_3: -20%

(a) Circuit X1

faults	deviation
f6	R_{A1}: -20%
f7	C_{A1}: +20%
f8	C_{B1}: -20%
f9	R_{C2}: +20%
f10	C_{C1}: +20%

(b) Circuit X2

faults	deviation
f11	R_1: +20%
f12	R_2: -20%
f13	R_3: -20%
f14	R_4: +20%
f15	R_7: -20%

(c) Circuit X3

Table 1 Fault list for circuit (a)X1 (b)X2 (c)X3

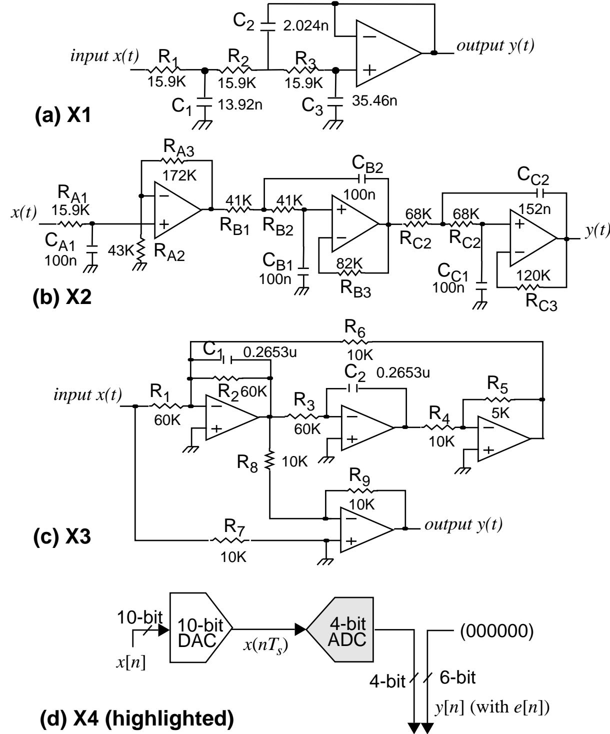

Fig.3(a)1KHz lowpass filter (b)100Hz lowpass filter (c)55-65Hz notch filter (d) 4-bit ADC

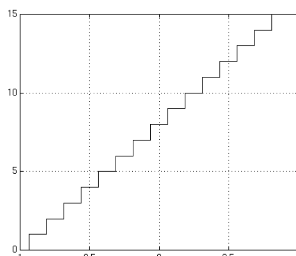

Fig4(a) fault-free

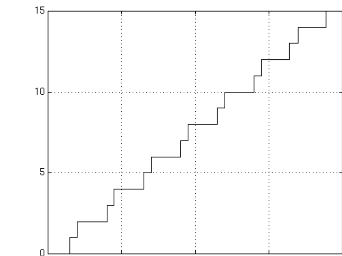

Fig4(b) Nonlinearity error (*f16*)

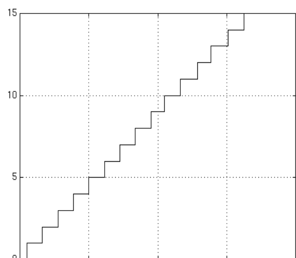

Fig4(b)Gain error (*f17*)

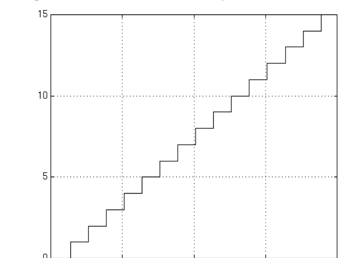

Fig4(b)Offset error (*f18*)

	R_{xy}[200]	R_{xy}[400]	R_{xy}[600]	R_{xy}[800]	R_{xy}[1000]	R_{xy}[1200]	R_y[0]	m_y
3σ	5.11	6.20	4.33	4.31	4.45	4.06	56.99	23.71
Δ_{f1}	-6.46	-4.18	0.61	3.61	4.14	2.59	-86.52	-0.17
Δ_{f2}	-6.12	-4.60	1.89	5.60	3.78	1.06	-82.03	-0.14
Δ_{f3}	10.42	-2.81	-12.72	-3.93	5.11	4.71	10.94	0.02
Δ_{f4}	12.49	-0.42	-13.92	-7.44	3.56	5.25	61.55	0.01
Δ_{f5}	8.69	-4.35	-11.10	-1.88	5.42	4.11	-15.40	<0.01

(a) Circuit X1 (*N*=128K)

	R_{xy}[2K]	R_{xy}[4K]	R_{xy}[6K]	R_{xy}[8K]	R_{xy}[10K]	R_{xy}[12K]	R_y[0]	m_y
3σ	6.55	9.23	12.75	12.56	7.40	6.73	128	0.021
Δ_{f6}	0.68	4.78	8.24	4.40	-4.23	-8.95	140	0.01
Δ_{f7}	-0.47	-3.54	-6.17	-4.51	1.90	6.38	-103	-0.005
Δ_{f8}	0.81	5.73	9.97	4.04	-8.74	-14.71	175	0.003
Δ_{f9}	0.59	4.22	3.64	-6.00	-11.58	-2.13	-68	-0.001
Δ_{f10}	-0.42	-3.16	-4.01	2.49	9.96	7.26	65	0.001

(b) Circuit X2 (*N*=256K)

	R_{xy}[6K]	R_{xy}[12K]	R_{xy}[18K]	R_{xy}[24K]	R_{xy}[30K]	R_{xy}[36K]	R_y[0]	m_y
3σ	7.96	8.49	11.87	12.47	7.42	8.28	124.27	0.027
Δ_{f11}	0.68	4.74	8.22	4.42	-4.21	-8.96	139.35	0.007
Δ_{f12}	-0.50	-3.52	-6.61	-4.52	1.88	6.37	-102.91	-0.005
Δ_{f13}	0.73	5.62	9.92	4.08	-8.68	-14.70	174.61	0.003
Δ_{f14}	0.47	4.26	3.76	-5.95	-11.66	-2.20	-66.62	-0.001
Δ_{f15}	0.45	3.73	2.47	-6.49	-10.12	-0.11	-83.10	0.001

(c) Circuit X3 (*N*=256K)

	R_{xy}[0]	R_{xy}[1]	R_{xy}[2]	R_{xy}[3]	R_y[0]	m_y
3σ	0.0075	0.0075	0.0072	0.0072	0.0075	0.0072
Δ_{f16}	-0.0103	-0.0106	-0.0106	-0.0106	-0.0199	-0.0213
Δ_{f17}	0.0287	0.0251	0.0252	0.0252	0.0609	0.0505
Δ_{f18}	-0.0159	-0.0164	-0.0164	-0.0164	-0.0309	-0.0330

(d) Circuit X4 (*N*=16K)

Table 2 Fault detection for $R_{xy}[m]$, R_y[0] and m_y

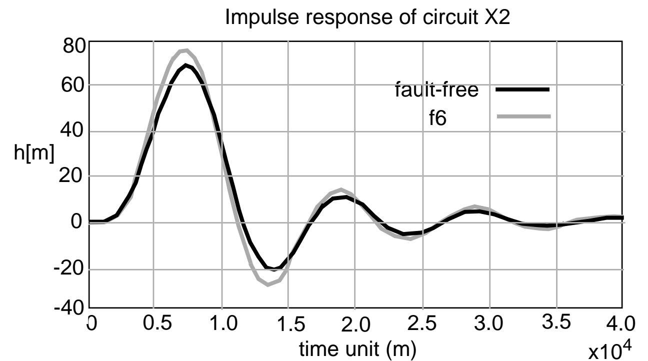

Fig.5 The impulse response for the fault-free and the faulty (*f6*) circuit X2